Epitaxial Growth of Pentacene on Alkali Halide Surfaces Studied by Kelvin Probe Force Microscopy

Julia L. Neff,[†,||] Peter Milde,[‡] Carmen Pérez León,[†,*] Matthew D. Kundrat,[§] Lukas M. Eng,[‡] Christoph R. Jacob,[§] and Regina Hoffmann-Vogel[†,*]

[†]Physikalisches Institut and DFG-Center for Functional Nanostructures, Karlsruhe Institute of Technology, Wolfgang-Gaede-Straße 1, 76131 Karlsruhe, Germany, [‡]Institut für Angewandte Photophysik, Technical University of Dresden, George-Baehr-Straße 1, 01069 Dresden, Germany, and [§]Institute of Physical Chemistry and DFG-Center for Functional Nanostructures, Karlsruhe Institute of Technology, Wolfgang-Gaede-Straße 1a, 76131 Karlsruhe, Germany. [||]Present address: Institut für Physikalische Chemie, Johannes Gutenberg-Universität Mainz, Duesbergweg 10-14, 55128 Mainz, Germany.

ABSTRACT In the field of molecular electronics, thin films of molecules adsorbed on insulating surfaces are used as the functional building blocks of electronic devices. Control of the structural and electronic properties of the thin films is required for reliably operating devices. Here, noncontact atomic force and Kelvin probe force microscopies have been used to investigate the growth and electrostatic landscape of pentacene on KBr(001) and KCl(001) surfaces. We have found that, together with molecular islands of upright standing pentacene, a new phase of tilted molecules appears near step edges on KBr. Local contact potential differences (LCPD) have been studied with both Kelvin experiments and density functional theory calculations. Our images reveal that differently oriented molecules display different LCPD and that their value is independent of the number of molecular layers. These results point to the formation of an interface dipole, which may be explained by a partial charge transfer from the pentacene to the surface. Moreover, the monitoring of the evolution of the pentacene islands shows that they are strongly affected by dewetting: Multilayers build up at the expense of monolayers, and in the Kelvin images, previously unknown line defects appear, which reveal the epitaxial growth of pentacene crystals.

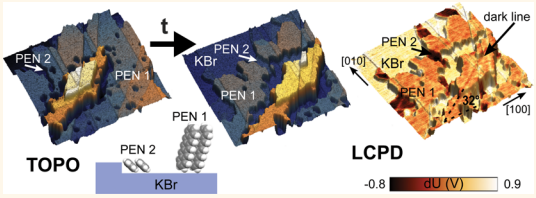

KEYWORDS: pentacene · epitaxial growth · dewetting · alkali halide · Kelvin probe force microscopy · noncontact atomic force microscopy · density functional theory calculations

Molecular electronics offers an alternative to conventional silicon electronics where individual or groups of molecules can be used as the functional building blocks of electronic devices. For a reliable functioning of such devices, it is necessary, on one hand, to decouple the electronic structure of the molecules from that of the substrate.[1] This can be achieved by using insulating surfaces as substrates, such as alkali halides.[2,3] On the other hand, control of the structural and electronic properties of the molecular layer, such as the surface electrostatic potential or dipoles, is required.[4−6] Of special interest is the initial stage of formation of thin films and their stability, *i.e.*, their dewetting properties.[7] The main techniques used for characterizing molecules on surfaces, such as photoemission and scanning tunneling microscopy, rely on the interaction of electrons with the surfaces. Thus, most studies have been limited to conductive surfaces. The development of scanning force microscopy has allowed identifying the structural properties of molecules on insulators.[8] Moreover, Kelvin probe force microscopy (KPFM) has the capability of detecting surface potential variations down to nanometer resolution.[9,10] In KPFM, a scanning force microscope is used to measure the electrostatic forces on the sample surface. For metals, these forces originate from work function differences between the tip and the sample. Applying an appropriate voltage to the sample or to the tip, the electrostatic forces can be minimized and the contact potential difference (CPD) determined. If the sample is covered by a thin overlayer of another material, the work function can change, *e.g.*, due to electron transfer and structural relaxation at the interface. Only recently has KPFM started to

* Address correspondence to carmen.perez.leon@kit.edu; r.hoffmann@kit.edu.

Received for review August 14, 2013 and accepted March 6, 2014.

Published online March 06, 2014
10.1021/nn404257v

be applied to insulating materials[11] and molecules deposited on bulk insulators.[12−14] On semiconducting or insulating materials, not only work function and ionization energy differences can cause such electrostatic forces but also localized charge, *e.g.*, from charge transfer or interface dipoles. Electrochemical equilibrium is reached when the Fermi level between the tip, the sample, and its back electrode is aligned. In the case of wide band gap insulators, such as alkali halide crystals, this equilibrium is reached only after long times such that the bulk Fermi level may not be well-defined.[15,16] Thus, the contact potential can vary from measurement to measurement.[12,16] Hence, it is more appropriate to focus on the variation of the contact potential difference along the surface (LCPD) rather than on its absolute value.[16]

In this work, we have investigated the geometric and electrostatic structure of pentacene islands on KBr(001) and KCl(001) surfaces by dynamic force microscopy and Kelvin probe force microscopy. Pentacene, among other organic molecules, has shown to be a promising p-type organic semiconductor that can be used to produce organic thin film transistors.[17] Our results reveal that besides the well-known phases of upright standing molecules, a phase of tilted pentacene is formed on some KBr samples. We also have found that differently oriented phases of the molecules cause different interface dipole or charge densities on the surface, which is discussed using density functional theory (DFT) calculations. The dewetting of the pentacene islands results in a change of the morphology of the islands, and mutilayers grow at the expense of monolayer islands. KPFM images reflect characteristic line defects on the islands. In monolayer islands, we ascribe them to domain boundaries, whereas in multilayer they indicate the growth direction of an epitaxial crystallization.

RESULTS AND DISCUSSION

Figures 1 and 2 show the KBr and KCl (001) surfaces after molecular deposition at room temperature. The majority of the islands display an apparent height of 1.65 ± 0.10 nm; see linecuts in Figures 1e and 2c. This length corresponds approximately to the length of a molecule, pointing to an upright standing configuration of pentacene (type 1 islands). The height measurements were cross-calibrated with the apparent height of substrate steps (0.33 nm for KBr(001) and 0.31 nm for KCl(001)) and determined from measurements where the electrostatic forces were compensated by using KPFM.[18] The islands grow across substrate step edges by shifting the molecular layer vertically without additional deformations detectable at this scale.

Previous works devoted to the growth of pentacene on alkali halides with X-ray diffraction, high-resolution electron diffraction, and AFM observed similar islands.[19−22] Our group has previously published

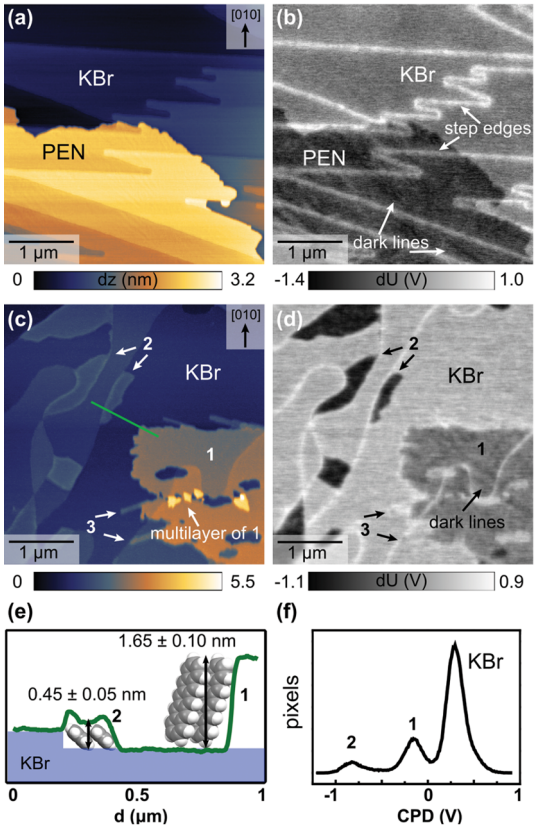

Figure 1. (a−d) Topography and corresponding Kelvin probe images of pentacene islands on KBr(001). (a and b) LCPD between the molecular islands, the alkali halide surface, and the substrate step edges are noticeable. γ = 0.08 fN$\sqrt{}$m. (c and d) Three different types of islands are distinguished. Type 1 is the same kind as the island in image (a) and (b). Type 2 and 3 display lower step heights. γ = 0.31 fN$\sqrt{}$m. (e) Line profile of the linecut in (c) that determines the topographic height of type 1 and 2 islands. (f) Histogram of the LCPD values in (d). The substrate orientation is indicated in the insets of (a) and (c).

high-resolution NC-AFM images of pentacene on KCl-(001).[22] Layers and islands of nearly upright standing molecules on the KBr(001)[19] and KCl(001) surfaces[19−21] have been reported in mainly two phases: the thin film[23,24] and the bulk phases.[25−27] While molecules in the thin film phase are oriented nearly perpendicular to the substrate, in the bulk phase they show a tilting angle of approximately 75°, thus displaying a slightly smaller height.[28,29]

Together with the islands of upright standing molecules, in some KBr samples a second type of island with a height of 0.45 ± 0.05 nm has been found (type 2), *e.g.*, Figure 1c and e. Owing to their reduced height, we assume that the pentacene molecules in these type 2 islands are arranged in a flat-lying or tilted fashion. On single-crystalline metal surfaces, such as Ag(111), Au(111), Cu(110), or HOPG, phases of flat-lying molecules are well known.[30−34] On HOPG this flat configuration is present only for submonolayer growth.[33] On KBr(001) and KCl(001) no strong interaction of the molecules with the surface is expected. Thus, we

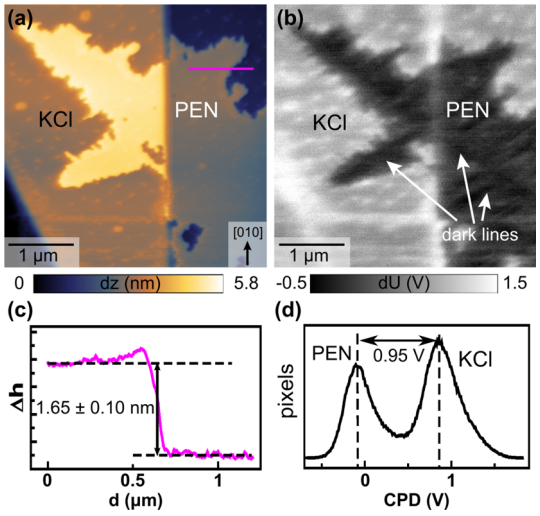

Figure 2. (a and b) Topography and corresponding Kelvin probe image of a pentacene island on KCl(001). γ = 0.24 fN$\sqrt{}$m. Also on KCl strong LCPD between the molecular islands, the alkali halide surface, and the substrate step edges are noticeable. (c) Line profile of the linecut in (a). (d) Histogram of the LCPD values in (b).

believe that the adsorbed molecules are arranged in a tilted fashion, probably forming rows of parallel molecules due to $\pi-\pi$ stacking, as suggested in the model in Figure 1e. This configuration is consistent with the measured apparent height of 0.45 nm and a tilting angle of approximately 30°, which agrees with the one found in the crystal structure of the bulk and thin film phases.[24−26] Type 2 islands do not grow over step edges but are confined on a terrace. They appear to extend aligned along the step edges. Presumably, they grow from the step edges of the terraces that are not exactly oriented along the ⟨100⟩ directions, which are the preferred orientations of the step edges on the (001) surfaces. Indeed, this type of island is observed only for the case in which the substrate has a large amount of higher indexed surface steps. This seems to be plausible, since it has been reported that molecular layers form special structures by confinement through substrate step edges.[35] The influence of the geometrical and electronic structure, *e.g.*, charge, of the higher indexed step edges should also be considered as an important determining factor.

A third kind of island with a stripe-like shape is additionally observed in the samples in which type 2 islands are present; two of them are marked with number 3 in Figure 1c. These islands display a similar apparent height to type 2 pentacene, making their classification ambiguous. In order to understand the nature of the different islands, Kelvin measurements have been analyzed.

KPFM images in Figure 1b and d and Figure 2b show that the type 1 and 2 molecular islands as well as the substrate step edges display a significant LCPD compared to the terraces. The strong Kelvin contrast at step edges has already been discussed in the literature:[11,36] Monovalent alkali halide type ionic crystals contain a small but noticeable amount of positively charged bivalent impurities such as Mg^{2+} or Ca^{2+}. These impurities are distributed evenly in the bulk crystal. The counterparts that maintain the charge neutrality are mostly anion vacancies, which gather at step edges at the surface, where their coordination is reduced. Thus, the step edges are negatively charged compared to the terraces, which corresponds to positive contrast in KPFM images following the description given by Barth *et al.*[11,13,36] On the contrary, type 1 and 2 pentacene islands appear darker than the terraces, meaning either that they are positively charged compared to the substrate or that a dipole moment is induced within the molecular layer or at the molecule−substrate interface, which points upward, *i.e.*, with a positive partial charge at the top of the pentacene layer and a negative partial charge close to the surface.

After analyzing the measured KPFM values we obtain that, on average, upright standing molecular islands on KBr (type 1) have an LCPD with respect to the crystal surface of approximately -0.45 ± 0.10 V, whereas the tilted ones (type 2) show an LCPD of -1.08 ± 0.10 V; see Figure 1f. On KCl, the LCPD between the upright standing molecules and the substrate is -0.95 ± 0.10 V; see Figure 2d. The magnitude of these LCPD is comparable to previous results of the adsorption of molecules on bulk insulators, *e.g.*, PTCDA on NaCl(001)[12] or triphenylene derivatives on KBr(001).[13] Type 3 islands, however, do not show any significant contact potential difference with respect to the substrate, apart from a bright contrast at their edges, as in the case of the alkali halide surface step egdes. Consequently, we ascribe such stripe-like protrusions to KBr islands produced by slightly overheating during preparation. The KPFM measurements permit us to unambiguously distinguish between differently oriented molecules, since they give rise to different LCPD values. This has also been observed for other molecules on metal[4,37] and insulating surfaces.[13]

It is important to understand where dipoles or charges are formed in order to find the origin of the different values of the LCPD. It is worth noticing that in the pentacene islands grown on KCl and KBr there is no difference between the LCPD measured on monolayers or on multilayers (see Figures 1c and 4). This means that the dominant process causing the change in LCPD occurs either at the first molecular layer due to an adsorption-induced polarization or at the interface between the pentacene and the alkali halide substrate owing to an interface dipole. Previous studies of pentacene on amorphous SiO_2 surfaces show differences in the LCPD between different layers, indicating a different behavior than in our system.[38] In the case of thin layers of insulating materials on metals, however, the LCPD was independent of the number of insulator layers, similar to our results.[39] Moreover, electric force

microscopy reports also ascribe the large contact potential differences between pentacene and SiO_2 to the formation of an interface dipole.[40]

To explore the possible origins of the LCPD, density functional theory calculations have been performed. First, the local charge distribution in unperturbed pentacene layers has been considered. As the simplest way of modeling the LCPD values, we have plotted the electrostatic potential on an isodensity surface (see Supporting Information for details). For type 1 islands, mainly the hydrogen atoms are probed by the tip, while for type 2 islands the aromatic π-system is exposed partly . In the latter case, a larger negative electrostatic potential due to the π-electrons should be observed. But this effect is opposite of the one found experimentally. Thus, the unperturbed local charge distributions in pentacene layers can be ruled out as responsible for the observed LCPD.

From the experimentally obtained LCPD values the interface dipole per molecule can be calculated using the Helmholtz equation:

$$\mu_{mol} = -\varepsilon_0 \Delta U_{CPD} A_{mol} \quad (1)$$

where A_{mol} is the surface area occupied by one molecule. For type 1 islands we obtain $\mu_{mol} = 9.53 \times 10^{-31}$ C m, assuming that the molecules are completely perpendicular to the surface, and $A_{mol} = ab/2 = 0.239$ nm^2 (a = 0.790 nm and b = 0.606 nm[25,26]). The tilted molecules (type 2) have a polarization of $\mu_{mol2} = 9.27 \times 10^{-30}$ C m; considering pentacene as a flat molecule, $A_{mol} = cb$ = 0.970 nm^2 (c = 1.601 nm[25,26]). Thus, the induced dipole moment in one pentacene molecule of type 2 islands is 1 order of magnitude larger than for the type 1.

We mentioned above that there are divalent impurities in the alkali halide's bulk and that negative charges are located at kink sites in order to compensate these charges.[11] Still, over the terraces this positive charge is not perfectly compensated and an electrostatic field is formed at the sample surface. This electric field can induce an interface dipole moment in the pentacene layer. The direction of the dipole moment induced by a positive background charge is consistent with the LCPD of the pentacene islands with respect to the alkali halide terraces. To estimate the induced dipole moments, the polarizability of a pentacene molecule has been calculated with time-dependent DFT (TDDFT). The polarizability of pentacene is strongly anisotropic, and its component perpendicular to the surface is twice as large for molecules in type 1 islands as for those in type 2 islands (see Supporting Information for details). Thus, one would expect type 1 islands to show a larger absolute LCPD than type 2 islands, which is not the case. Moreover, the adsorption-induced polarization should become larger for multilayers of pentacene, which is not observed experimentally. Hence, an adsorption-induced polarization cannot explain the measured LCPD.

This leaves an interface dipole between the molecules and the surface as the remaining explanation for the observed LCPD. The apparent positive charge of the pentacene islands compared to the surface is consistent with a partial transfer of electrons from the pentacene molecules to the surface, which is in line with the low ionization potential of pentacene. Using the dipole moments per molecule determined from the LCPD and assuming a separation of 0.5 nm between the partial positive charge in the pentacene molecule and a partial negative countercharge at the surface, this would require the transfer of a partial charge of 0.012 e per pentacene molecule in type 1 islands and of 0.118 e per pentacene molecule in type 2 islands. Considering that in type 2 islands this charge can be distributed over the whole π-system, while in type 1 islands it has to be localized close to the surface, these values appear reasonable. Such a charge transfer at the molecule−surface interface is also consistent with the observation that the LCPD is unchanged for multilayers. Verifying this explanation of the LCPD with DFT calculations would require modeling both the molecular layers and the alkali halide surface, which we did not attempt here.

The stability of the pentacene layer is an important issue for practical applications; therefore we have investigated the evolution and changes of the molecular islands' morphology on the time scale of hours to days. We observe that the pentacene adsorbed on the alkali halide (001) surfaces suffers from after-deposition dewetting. Dewetting is known to be driven by strain in the molecular layer, which may be released by changing its internal structure.[7] These changes lead to three different visible effects: (1) The substructure of monolayer islands gets more pronounced; (2) the island edges and the area near the edges break and holes appear; (3) multilayers build up at the expense of monolayers.

When scanning with low cantilever amplitudes, a substructure becomes visible on the molecular islands. This substructure gets more pronounced with time, especially for the islands grown on the KCl(001) surface. Figure 3 shows islands several days after deposition. The substructure consists of many line-shaped features organized in some kind of domains with different orientations; see Figure 3a−c. In each domain the substructure lines point to similar directions, which are not randomly oriented but seem to show some preferred angles, as indicated by the given angles in Figure 3.

The morphology of the island edges is also affected by dewetting: the borders fray and holes break, as it can be seen in the images of Figure 3. The holes do not break randomly, but their position is correlated with the position of surface defects. Different surface defects have been found on the alkali halide surfaces owing to small differences in the preparation conditions. Typically alkali halides show wedge-shaped

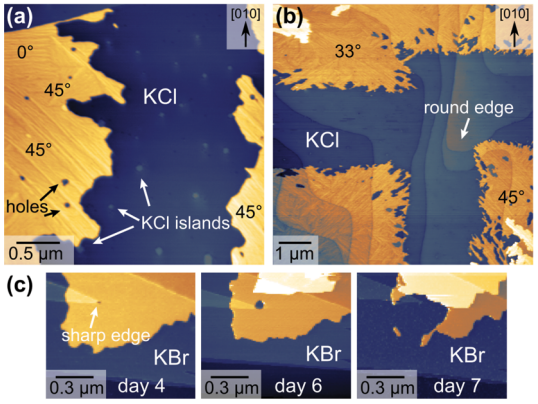

Figure 3. Dewetting of pentacene islands on (a and b) KCl(001) after 5 and 8 days, respectively. (c) KBr(001) monitored over several days. The borders of the islands fray and holes appear, mainly where defects such as step edges or small substrate islands are present. (a) γ = 0.15 fN$\sqrt{}$m. (b) γ = 0.09 fN$\sqrt{}$m. (c) γ = 0.04 fN$\sqrt{}$m.

terraces with sharp edges, while slight overheating of the substrate results in round terraces and small islands on top of them. Figure 3 illustrates the role of the different defects: On surfaces with round step edges and KCl islands, such as in Figure 3a and b, the holes break preferably above the small islands. On samples with clean, wedge-shaped terraces holes appear only at the sharp edge of the terrace, as indicated in Figure 3c. In Figure 3b the initial shape of the molecular island is still recognizable: the islands were aligned with the ⟨100⟩ directions of the KCl substrate. On such islands, holes typically elongate along the directions of the substructure of the pentacene islands. Owing to these holes, the island's shape modifies into a fractal-like geometry. Such a change of the island morphology toward dendritic structures has also been observed for pentacene on SiO_2 in thermally activated dewetting experiments.[41]

The third change in the topography is the formation of multilayers. In Figure 3c we can see how a second layer grows while the lower layer decreases in size (*i.e.*, the hole increases in size). In Figure 4a and c dewetted islands with multilayer structure are presented (see Supporting Information for details). The transformation of monolayers into higher-layered islands is a common way of dewetting of molecules on alkali halide surfaces[7] and has already been observed on pentacene adsorbed on other insulating surfaces.[42]

The dewetting behavior of type 2 pentacene islands is rather different than that of type 1 islands. Their borders do not change much, their topography and Kelvin contrast do not vary, neither do they form multilayers. Some of the small islands surrounded by type 1 islands disappear or are "absorbed" by the growth of the multilayer, as we can see in Figure 4. Besides this, the isolated islands become enlarged along the high-indexed step edges at which they grow and remain more or less stable in time, as shown in Figure 5. See Supporting Information for details.

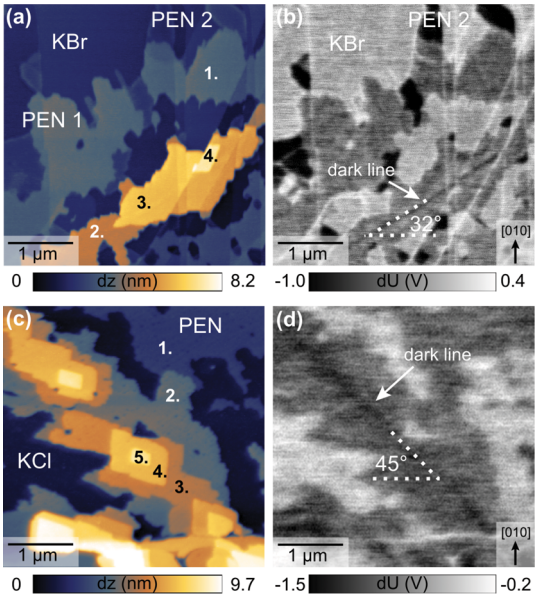

Figure 4. Topography and corresponding Kelvin probe image of the dewetting of pentacene islands on (a and b) KBr(001) after 2 days. γ = 0.05 fN$\sqrt{}$m. (c and d) KCl(001) after 4 days. γ = 0.56 fN$\sqrt{}$m. Surprisingly, there are no differences in the LCPD of multilayers and monolayers. A dark line at the center of the multilayer island is revealed in the Kelvin probe images.

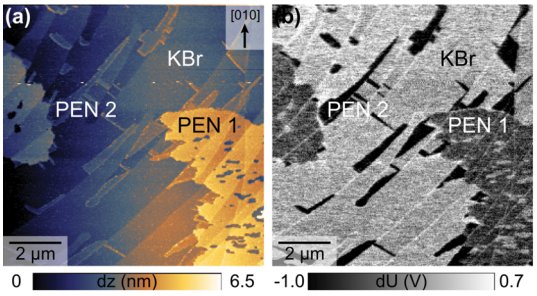

Figure 5. (a and b) Topography and corresponding Kelvin probe image of the dewetting of pentacene type 2 islands on KBr(001) after 3 days. γ = 0.08 fN$\sqrt{}$m.

Further insight into the dewetting process is gained by analyzing the Kelvin probe data. Figure 4 displays the simultaneously obtained topographic and KPFM data of dewetted molecular islands on KBr and KCl. In Figure 4a and b, type 1 and type 2 islands of the differently oriented molecules reported above are clearly distinguished. In addition, a new feature is observed in the surface potential of the multilayer island that is not correlated with any visible topographic change on the surface, at least not in the surface of the upper layer: a dark line crosses the island. A similar line is observed in Figure 4d.

On monolayer islands much weaker dark lines are observed in the KPFM images, and a few examples are indicated by arrows in Figure 1b and d and Figure 2b. These weak dark lines are distributed on the islands and in some cases run parallel to the axis of the islands; for example, in Figure 2 one line runs along the main

axis, and many others run perpendicular to it. However, in multilayers the dark line in the middle of the island is the predominant feature. For the sake of clarifying its role, a thorough analysis of such lines has been done on all acquired data on dewetted multilayer islands. Taking into account a margin of error owing to drift in our scans, the results show that the dark lines always run along the middle axis of the island and that they follow preferred orientations. The angles of such orientations with respect to the [100] axis correspond to 33° and 45° for pentacene islands on KBr, and 0°, 33°, and 45° on KCl, and their equivalent directions. Examples are given in Figure 4b and d. These angles also coincide with the ones followed by the substructure lines observed in the topography (shown in Figure 3).

The dark lines of multilayers islands therefore indicate the epitaxial relationship between the forming pentacene microcrystals and the substrate. Furthermore, in Figure 4c, the alignment on the second-layer (and higher) islands is identical, evidencing that they mimic the structure of the underlying island; that is, the higher layers of pentacene grow epitaxially with respect to the first one.[43] Typically pentacene crystals grow with a rhomboid shape with two perpendicular axes.[43] These axes have been associated with the herringbone structure characteristic on pentacene crystals and its polymorphs.[43] The fact that the island's orientation follows preferred directions indicates an epitaxial growth of pentacene on the KBr and KCl (001) surfaces. The angles 0° and 90° may correspond to nucleation controlled at step edges in which the growth direction is given by the orientation of the step edge. Angles of 33° may correspond to a point-on-line epitaxy of the pentacene molecular crystal with respect to the alkali halide surface, confirming the observation of Kiyomura *et al.*[19,20] Finally, 45° may correspond to nucleation along one of the major crystallographic surface directions. See Supporting Information for details.

Throughout this paper, we have discussed that the Kelvin contrast arises from the interface of alkali halide−molecules owing to the formation of an interface dipole. The LCPD value of the dark lines is larger than the one of type 1 islands but lower than that of type 2 islands. According to the earlier analysis, the LCPD originates from a partial charge transfer from the pentacene molecules to the surface. Since the charge is differently distributed for distinct molecular orientations, different LCPD are observed for distinct molecular phases. This suggests a different arrangement of the pentacene molecules along the dark lines. Additionally, charge accumulation due to trapped charges can occur in such areas, since the presence of mobile charge carriers has been demonstrated.[44] Consequently, we can explain the weak dark lines in the monolayer islands as domain boundaries, where the molecules may be differently oriented. This is consistent with the appearance of a substructure in the topography and with the previous observation of domain boundaries in molecularly resolved images.[22] On newly formed multilayer islands, the strong dark lines along their middle axis, however, are not expected to be correlated with a domain boundary. Their origin is therefore not straightforward to explain. We tentatively ascribe them to nucleation seeds of the new crystal, where different pentacene orientations, interactions with the substrate surface, or charge accumulation occurs. This would explain their relation with the epitaxial growth of the microcrystals.

CONCLUSIONS

We have investigated the growth and dewetting properties of pentacene on alkali halide surfaces. We have found that together with islands of upright standing molecules a new phase of lying-tilted pentacene appears on KBr samples with a large amount of high indexed surface steps, probably due to confinement. All molecular islands display strong LCPD compared to the substrate owing to a partial transfer of electrons from the molecules to the insulating surface. The charge is differently distributed for distinct molecular orientations, leading to different LCPD values.

Insight into the crystallization process is gained by observing the temporal evolution of the islands. Induced by dewetting, the molecules rearrange, modifying the islands' topography, including a transformation of the two-dimensional monolayers into three-dimensional microstructures. The analysis of the data unveils an epitaxial growth of the pentacene on alkali halide surfaces. The new multilayer islands display a new feature in the KPFM images: a dark line that runs along their middle axis. We relate such a line to the epitaxial growth of the pentacene crystal and tentatively explain its contrast by accumulated charge.

Summarizing, the monitoring of the crystallization process of pentacene with NC-AFM and KPFM reveals that not only the geometrical arrangement of the molecules is influenced but also the electronic properties.

METHODS

Experimental Details. The sample preparation and measurements were carried out in an ultra-high-vacuum chamber with a base pressure of less than 3×10^{-10} mbar. Atomically clean KBr and KCl (001) surfaces were obtained by cleaving single crystals in air, immediately introducing the crystals to the vacuum chamber, and heating them to about 400 K for 1 h. The pentacene molecules were thermally deposited onto the substrates after degassing the molecular source for several hours at temperatures slightly below the sublimation temperature (508 K). Samples were then transferred to an Omicron scanning

force microscope (Omicron NanoTechnology GmbH, Germany) equipped with Nanosensors cantilevers (Neuchatel, Switzerland) and a Nanonis phase-locked loop electronics (SPECS, Switzerland). All measurements were carried out in the noncontact mode, where the tip is oscillated at an amplitude of a few nanometers, kept constant by a feed-back loop at resonance. The resonance frequency of the cantilever is measured as it reduces when the tip is approached to the sample surface under the influence of the interaction of tip and surface. Topographical imaging is carried out at constant frequency shift using cantilevers with a force constant of 40 N/m and a free resonance frequency of 170 kHz. For Kelvin probe measurements performed in parallel to the topography measurements, the voltage applied to the tip was oscillated with a frequency of 2 kHz and an amplitude of 3 V (frequency-modulation-mode of KPFM). For these measurements, cantilevers with a platinum–iridium-coated tip, a force constant of 3 N/m, and a free resonance frequency of 75 kHz were used. For characterizing the NC-AFM images the normalized frequency shift has been used: $\gamma = \Delta f k A^{3/2}/f_0$. In order to fulfill the description given by Barth *et al.*,[11] *i.e.*, negative charge shows positive contrast, the contrast of the KPFM images has been inverted.

Computational Details. DFT calculations were performed with the Amsterdam Density Functional (ADF) program package.[45,46] The BLYP exchange–correlation functional[47,48] was used in conjunction with the TZ2P Slater-type basis set.[49]

Conflict of Interest: The authors declare no competing financial interest.

Acknowledgment. We thank the European Research Council for financial support through the starting grant NANOCONTACTS (No. ERC 2009-Stg 239838) and M. Marz for fruitful discussions.

Supporting Information Available: Local charge distribution and polarizability of pentancene; dewetting of pentacene; and point-on-line epitaxy of pentacene on KBr and KCl. This material is available free of charge *via* the Internet at http://pubs.acs.org.

REFERENCES AND NOTES

1. Such, B.; Trevethan, T.; Glatzel, T.; Kawai, S.; Zimmerli, L.; Meyer, E.; Shluger, A. L.; Amijs, C. H. M.; de Mendoza, P.; Echavarren, A. M. Functionalized Truxenes: Adsorption and Diffusion of Single Molecules on the KBr(001) Surface. *ACS Nano* **2010**, *4*, 3429–3439.
2. Repp, J.; Meyer, G. Molecules on Insulating Films: Scanning-Tunneling Microscopy Imaging of Individual Molecular Orbitals. *Phys. Rev. Lett.* **2005**, *94*, 026803.
3. Ramoino, L.; von Arx, M.; Schintke, S.; Baratoff, A.; Guntherodt, H.-J.; Jung, T. A. Layer-Selective Epitaxial Self-Assembly of Porphyrins on Ultrathin Insulators. *Chem. Phys. Lett.* **2006**, *417*, 22–27.
4. Nikiforov, M. P.; Zerweck, U.; Milde, P.; Loppacher, C.; Park, T.-H.; Uyeda, H. T.; Therien, M. J.; Eng, L.; Bonnell, D. The Effect of Molecular Orientation on the Potential of Porphyrin-Metal Contacts. *Nano Lett.* **2008**, *8*, 110–113.
5. Berkebile, S.; Koller, G.; Fleming, A. J.; Puschnig, P.; Ambrosch-Draxl, C.; Emtsevc, K.; Seyller, T.; Rileyd, J.; Ramsey, M. G. The Electronic Structure of Pentacene Revisited. *J. Electron Spectrosc. Relat. Phenom.* **2009**, *174*, 22–27.
6. Liu, S.; Wang, W. M.; Briseno, A. L.; Mannsfeld, S. C. E.; Bao, Z. Controlled Deposition of Crystalline Organic Semiconductors for Field-Effect-Transistor Applications. *Adv. Mater.* **2009**, *21*, 1217–1232.
7. Burke, S. A.; Topple, J. M.; Grütter, P. Molecular Dewetting on Insulators. *J. Phys.: Condens. Matter* **2009**, *21*, 423101.
8. Gross, L.; Mohn, F.; Moll, N.; Liljeroth, P.; Meyer, G. The Chemical Structure of a Molecule Resolved by Atomic Force Microscopy. *Science* **2009**, *325*, 1110.
9. Nonnenmacher, M.; Oboyle, M. P.; Wickramasinghe, H. K. Kelvin Probe Force Microscopy. *Appl. Phys. Lett.* **1991**, *58*, 2921–2923.
10. Mohn, F.; Gross, L.; Moll, N.; Meyer, G. Imaging the Charge Distribution within a Single Molecule. *Nat. Nanotechnol.* **2012**, *7*, 227–231.
11. Barth, C.; Henry, C. R. Surface Double Layer on (001) Surfaces of Alkali Halide Crystals: A Scanning Force Microscopy Study. *Phys. Rev. Lett.* **2007**, *98*, 136804.
12. Burke, S. A.; LeDue, J. M.; Miyahara, Y.; Topple, J. M.; Fostner, S.; Grütter, P. Determination of the Local Contact Potential Difference of PTCDA on NaCl: A Comparison of Techniques. *Nanotechnology* **2009**, *20*, 264012.
13. Hinaut, A.; Pujol, A.; Chaumeton, F.; Martrou, D.; Gourdon, A.; Gauthier, S. An NC-AFM and KPFM Study of the Adsorption of a Triphenylene Derivative on KBr(001). *Beilstein J. Nanotechnol.* **2012**, *3*, 221–229.
14. Kittelmann, M.; Rahe, P.; Gourdon, A.; Kühnle, A. Direct Visualization of Molecule Deprotonation on an Insulating Surface. *ACS Nano* **2012**, *6*, 7406–7411.
15. Barth, C.; Hynninen, T.; Bieletzki, M.; Henry, C. R.; Foster, A. S.; Esch, F.; Heiz, U. AFM Tip Characterization by Kelvin Probe Force Microscopy. *New J. Phys.* **2010**, *12*, 093024.
16. Sadeghi, A.; Baratoff, A.; Ghasemi, S. A.; Goedecker, S.; Glatzel, T.; Kawai, S.; Meyer, E. Multiscale Approach for Simulations of Kelvin Probe Force Microscopy with Atomic Resolution. *Phys. Rev. B* **2012**, *86*, 075407.
17. Kitamura, M.; Arakawa, Y. Pentacene-Based Organic Field-Effect Transistors. *J. Phys.: Condens. Matter* **2008**, *20*, 184011.
18. Sadewasser, S.; Lux-Steiner, M. C. Correct Height Measurement in Noncontact Atomic Force Microscopy. *Phys. Rev. Lett.* **2003**, *91*, 266101.
19. Kiyomura, T.; Nemoto, T.; Yoshida, K.; Minari, T.; Kurata, H.; Isoda, S. Epitaxial Growth of Pentacene Thin-Film Phase on Alkali Halides. *Thin Solid Films* **2006**, *515*, 810–813.
20. Kiyomura, T.; Nemoto, T.; Ogawa, T.; Minari, T.; Yoshida, K.; Kurata, H.; Isoda, S. Thin-Film Phase of Pentacene Film Formed on KCl by Vacuum Deposition. *Jap. J. Appl. Phys.* **2006**, *45*, 401–404.
21. Kakudate, T.; Yoshimoto, N.; Kawamura, K.; Saito, Y. Observation of Epitaxial Growth of Pentacene Thin Films on KCl Substrate by X-Ray Diffractometry. *J. Cryst. Growth* **2007**, *306*, 27–32.
22. Neff, J. L.; Götzen, J.; Li, E.; Marz, M.; Hoffmann-Vogel, R. Molecular-Resolution Imaging of Pentacene on KCl(001). *Beilstein J. Nanotechnol.* **2012**, *3*, 186–191.
23. Yoshida, H.; Inaba, K.; Sato, N. X-Ray Diffraction Reciprocal Space Mapping Study of the Thin Film Phase of Pentacene. *Appl. Phys. Lett.* **2007**, *90*, 181930.
24. Nabok, D.; Puschnig, P.; Ambrosch-Draxl, C.; Werzer, O.; Resel, R.; Smilgies, D.-M. Crystal and Electronic Structures of Pentacene Thin Films from Grazing-Incidence X-Ray Diffraction and First-Principles Calculations. *Phys. Rev. B* **2007**, *76*, 235322.
25. Campbell, R. B.; Robertson, J. M.; Trotter, J. Crystal and Molecular Structure of Pentacene. *Acta Crystallogr.* **1961**, *14*, 705–711.
26. Campbell, R. B.; Robertson, J. M.; Trotter, J. Crystal Structure of Hexacene, and a Revision of Crystallographic Data for Tetracene and Pentacene. *Acta Crystallogr.* **1962**, *15*, 289–290.
27. Siegrist, T.; Kloc, C.; Schön, J. H.; Batlogg, B.; Haddon, R. C.; Berg, S.; Thomas, G. A. Enhanced Physical Properties in a Pentacene Polymorph. *Angew. Chem., Int. Ed.* **2001**, *40*, 1732–1736.
28. Mattheus, C. C.; Dros, A. B.; Baas, J.; Oostergetel, G. T.; Meetsma, A.; de Boer, J. L.; Palstra, T. T. Identification of Polymorphs of Pentacene. *Synth. Met.* **2003**, *138*, 475–481.
29. Ambrosch-Draxl, C.; Nabok, D.; Puschnig, P.; Meisenbichler, C. The Role of Polymorphism in Organic Thin Films: Oligoacenes Investigated from First Principles. *New J. Phys.* **2009**, *11*, 125010.
30. Lukas, S.; Witte, G.; Wöll, C. Novel Mechanism for Molecular Self-Assembly on Metal Substrates: Unidirectional Rows of Pentacene on Cu(110) Produced by a Substrate-Mediated Repulsion. *Phys. Rev. Lett.* **2001**, *88*, 028301.

31. France, C. B.; Schroeder, P. G.; Forsythe, J. C.; Parkinson, B. A. Scanning Tunneling Microscopy Study of the Coverage-Dependent Structures of Pentacene on Au(111). *Langmuir* **2003**, *19*, 1274–1281.
32. Käfer, D.; Ruppel, L.; Witte, G. Growth of Pentacene on Clean and Modified Gold Surfaces. *Phys. Rev. B* **2007**, *75*, 085309l.
33. Götzen, J.; Käfer, D.; Wöll, C.; Witte, G. Growth and Structure of Pentacene Films on Graphite: Weak Adhesion As a Key for Epitaxial Film Growth. *Phys. Rev. B* **2010**, *81*, 085440.
34. Götzen, J.; Lukas, S.; Birkner, A.; Witte, G. Absence of Template Induced Ordering in Organic Multilayers: The Growth of Pentacene on a Cu(221) Vicinal Surface. *Surf. Sci.* **2011**, *605*, 577–581.
35. Nony, L.; Gnecco, E.; Baratoff, A.; Alkauskas, A.; Bennewitz, R.; Pfeiffer, O.; Maier, S.; Wetzel, A.; Meyer, E.; Gerber, C. Observation of Individual Molecules Trapped on a Nanostructured Insulator. *Nano Lett.* **2004**, *4*, 2185–2189.
36. Egberts, P.; Filleter, T.; Bennewitz, R. A Kelvin Probe Force Microscopy of Charged Indentation-Induced Dislocation Structures in KBr. *Nanotechnology* **2009**, *20*, 264005.
37. Milde, P.; Zerweck, U.; Eng, L. M.; Abel, M.; Giovanelli, L.; Nony, L.; Mossoyan, M.; Porte, L.; Loppacher, C. Interface Dipole Formation of Different ZnPcCl(8) Phases on Ag(111) Observed by Kelvin Probe Force Microscopy. *Nanotechnology* **2008**, *19*, 305501.
38. Kalihari, V.; Ellison, D. J.; Haugstad, G.; Frisbie, C. D. Observation of Unusual Homoepitaxy in Ultrathin Pentacene Films and Correlation with Surface Electrostatic Potential. *Adv. Mater.* **2009**, *21*, 3092–3098.
39. Loppacher, C.; Zerweck, U.; Eng, L. M. Kelvin Probe Force Microscopy of Alkali Chloride Thin Films on Au(111). *Nanotechnology* **2004**, *15*, S9.
40. Chen, L.; Ludeke, R.; Cui, X.; Schrott, A. G.; Kagan, C. R.; Brus, L. E. Electrostatic Field and Partial Fermi Level Pinning at the Pentacene-SiO_2 Interface. *J. Phys. Chem. B* **2005**, *109*, 1834–1838.
41. Käfer, D.; Wöll, C.; Witte, G. Thermally Activated Dewetting of Organic Thin Films: the Case of Pentacene on SiO_2 and Gold. *Appl. Phys. A: Mater. Sci. Process.* **2009**, *95*, 273–284.
42. Amassian, A.; Pozdin, V. A.; Desai, T. V.; Hong, S.; Woll, A. R.; Ferguson, J. D.; Brock, J. D.; Malliarasa, G. G.; Engstrom, J. R. Post-Deposition Reorganization of Pentacene Films Deposited on Low-Energy Surfaces. *J. Mater. Chem.* **2009**, *19*, 5580–5592.
43. Ruiz, R.; Nickel, B.; Koch, N.; Feldman, L. C.; Haglund, R. F.; Kahn, A.; Scoles, G. Pentacene Ultrathin Film Formation on Reduced and Oxidized Si Surfaces. *Phys. Rev. B* **2003**, *67*, 125406.
44. Jiang, Y.; Qi, Q.; Wang, R.; Zhang, J.; Xue, Q.; Wang, C.; Jiang, C.; Qiu, X. Direct Observation and Measurement of Mobile Charge Carriers in a Monolayer Organic Semiconductor on a Dielectric Substrate. *ACS Nano* **2011**, *5*, 6195–6201.
45. te Velde, G.; Bickelhaupt, F. M.; Baerends, E. J.; Fonseca Guerra, C.; van Gisbergen, S. J. A.; Snijders, J. G.; Ziegler, T. Chemistry with ADF. *J. Comput. Chem.* **2001**, *22*, 931.
46. ADF, Amsterdam Density Functional Program, 2012. URL: http://www.scm.com.
47. Becke, A. D. Density-Functional Exchange-Energy Approximation with Correct Asymptotic Behavior. *Phys. Rev. A* **1988**, *38*, 3098.
48. Lee, C.; Yang, W.; Parr, R. G. Development of the Colle-Salvetti Correlation-Energy Formula into a Functional of the Electron Density. *Phys. Rev. B* **1988**, *37*, 785.
49. van Lenthe, E.; Baerends, E. J. Optimized Slater-Type Basis Sets for the Elements. *J. Comput. Chem.* **2003**, *24*, 1142.